Automated selection of suitable atmospheric calibration sites for satellite imagery

R. T. Wilson and E. J. Milton

School of Geography, University of Southampton, Southampton, UK, SO17 1BJ
Email: rtw1v07@soton.ac.uk

Abstract

Ground calibration targets (GCTs) play a vital role in atmospheric correction of satellite sensor data in the optical region, but selecting suitable targets is a subjective and time-consuming task. This paper describes a method to automatically select suitable GCTs, using a combination of remotely sensed multispectral and topographic data. Desirable characteristics for GCTs sites were identified from the literature, and used to devise a semi-automated workflow based on programs written in IDL combined with routines offered by ITTVIS ENVI and Definiens eCognition. Spatial statistics were used to assess local patterns of spatial uniformity, and endmember abundances (extracted using the SMACC algorithm) were used in a novel method to ensure a spread of calibration sites throughout the brightness range for each band. The result of this process was a map of candidate GCTs, classified according to their suitability.

1 Introduction

Ground calibration targets (GCTs) are used in the empirical line method (ELM) of atmospheric correction (Smith and Milton, 1999), for vicarious calibration of satellite and aircraft sensors (Thome, 2001; Secker et al., 2001), for validation of atmospheric correction methods based on radiative transfer (RT) models (Holm et al., 1989), and in hybrid approaches to atmospheric correction (Clark et al., 2003). Furthermore, if the spectral properties of GCTs are stable over time they can be considered as samples from a class of image objects known as ‘pseudo-invariant features’ (PIF) (Schott et al., 1988), which may be used for normalising a time series of images (Schmidt et al., 2008).

GCTs may be defined statistically, based on the properties of the image data (Elvidge et al., 1995; Canty and Nielsen, 2008) or real-world objects may be used, such as unvegetated areas or artificial surfaces (Caselles and Garcia, 1989). For relative normalisation of several images, statistically-derived GCTs may suffice, but if it is necessary to convert an image to reflectance it is generally necessary to use real-world target whose spectral properties can be characterised using field spectroscopy. In this case there is debate in the literature between those who argue for use of a large number of GCTs covering a range of reflectance and distributed across the image (Karpouzli and Malthus, 2003) and those who favour more detailed investigation of a single bright target (Moran et al., 2001). Identifying such GCTs is a time-consuming and subjective process, so the aim of this study was to produce an automated method to select areas that meet the basic criteria for a good GCT for use with all methods of empirical atmospheric correction (Table 1).

Table 1 - Overview of the desirable characteristics of GCTs (Smith and Milton, 1999, Karpouzli and Malthus, 2003)

Criterion	Justification
Large	Minimises the effect of the point spread function. Slater (1980) recommends an area at least 8x the nominal pixel size.
Range of reflectances	Avoids extrapolating the regression line beyond the limits of the GCT data. Mid-range reflectance GCTs are also useful to check the linearity of the relationship.
Stable over time	Few if any GCTs are spectrally invariant over time, but the changes in some surfaces can be accounted for by use of a BRDF model (Moran et al., 2001).
Spatially homogenous	Reduces the importance of positional accuracy in the ground measurements and minimises the effect of image misregistration. Reduces the probability of mixed pixels occurring.
Flat	Reduces the importance of the time of image acquisition.
Sites spread throughout the image	Ensures the variation in atmospheric conditions across the image to be accounted for.

2 Method

The study focused on data from SPOT-5 HRG as its 10 metre nominal spatial resolution and spectral bands in visible and near infra-red wavelengths mean that it is well-suited to land cover mapping in Europe.

2.1 Processing and thresholding

IDL code was written within the ENVI environment to automate the steps described below. Getis-Ord statistics (Getis, 1994) were used to measure spatial uniformity, as this has been shown to be more sensitive to small-scale variations than the co-efficient of variation (Bannari et al., 2005). Large magnitude positive values show bright uniform areas, and large magnitude negative values show dark uniform areas. A novel method was used to ensure the selected calibration sites were some of the darkest and brightest pixels in each band. GCTs were selected which were close to the endmembers of the image, as this ensures they are close to the edges of the pixel cloud, and therefore the minima and maxima of the image. The SMACC algorithm (Gruninger et al., 2004) was used, and was set to output abundance images for five endmembers. The images produced in the previous two stages were converted to a binary image masks by selecting the top and bottom 0.3% of the Getis-Ord images and the top 0.3% of the endmember abundance images. These thresholds were empirically derived.

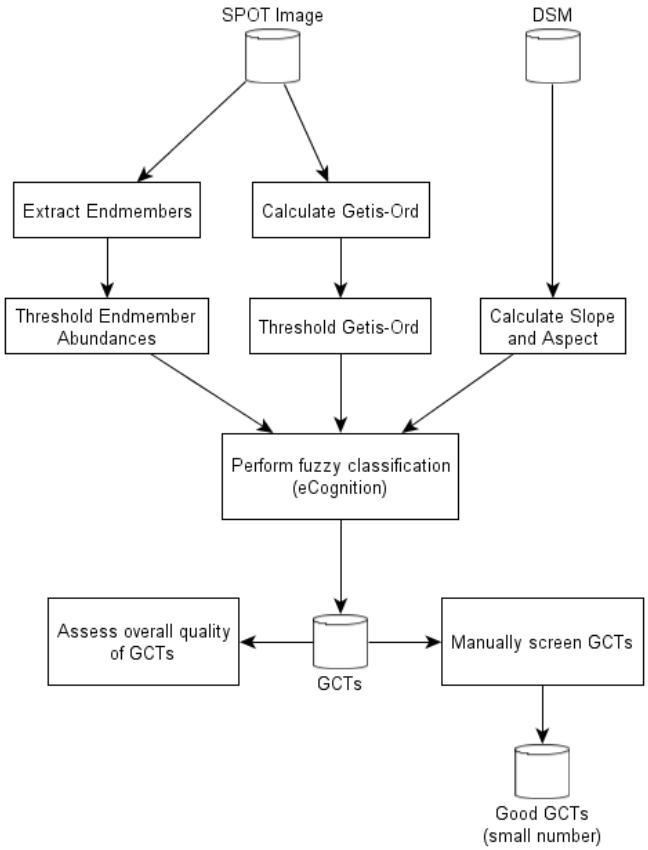

Figure 1 - Overview of the method

2.2 Site selection

This was performed using fuzzy object-based classification in Definiens eCognition version 4. The image was segmented at two levels and classified according to a set of rules (shown in *Figure 2*). The *Customised Feature* function in eCognition was used to allow rules to be created based on the percentage of the image object selected in the binary masks derived above. When studying the images it was found that a number of buildings had sawtooth roofs. These are unsuitable for use as GCTs as their reflectance varies considerably with changes in Sun angle. These were excluded by a rule checking the coefficient of variation of an aspect image created from the DSM. It was found that this rule worked even when the sawtooths had a periodicity less than the resolution of the sensor..

2.3 Refining the site selection

The selected sites were then subjected to a second stage of screening as to their suitability for the specific application. In the present study this stage was performed manually.

3 Data sources

A SPOT-5 HRG half-scene (029/246) centred on 51º 12'N, 1º 27'W was acquired by CNES on 10th June 2006 in support of the NCAVEO Field Campaign (Milton et al., 2008), and a subset 7.3km x 5.4km centred on the town of Andover, Hampshire was used in this study (Figure 3). The digital surface model was derived from an interferometric synthetic aperture

radar (IFSAR) survey undertaken by Intermap Technologies (NEXTMap Britain) and had an estimated vertical precision of 30cm.

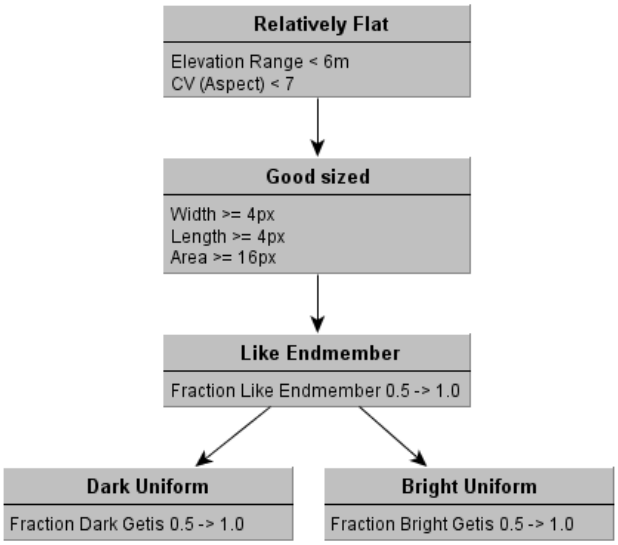

Figure 2 - Rules used for object-based classification in eCognition

4 Results

Figure 3 shows the candidate GCTs on the SPOT image, identified by numbers which will be used in the discussion below.

Figure 3 - SPOT HRG image showing dark GCTs in yellow and bright GCTs in magenta

Figure 4 shows that the selected GCTs cover the three vertices of the pixel cloud very well, and therefore the site selection procedure is producing good candidate GCTs for this image.

3.1 Dark GCT

All the dark GCT selected by the automated method were water bodies, so the data from all four were merged. The composite water class was positively skewed, especially in the near infra-red band; this is thought to have arisen from aquatic macrophytes which were visible in some of the lakes. In order to purify the water class, the 30 pixels within the candidate water GCT having the lowest near infra-red values were identified, and the median of these was taken to represent the definitive dark GCT.

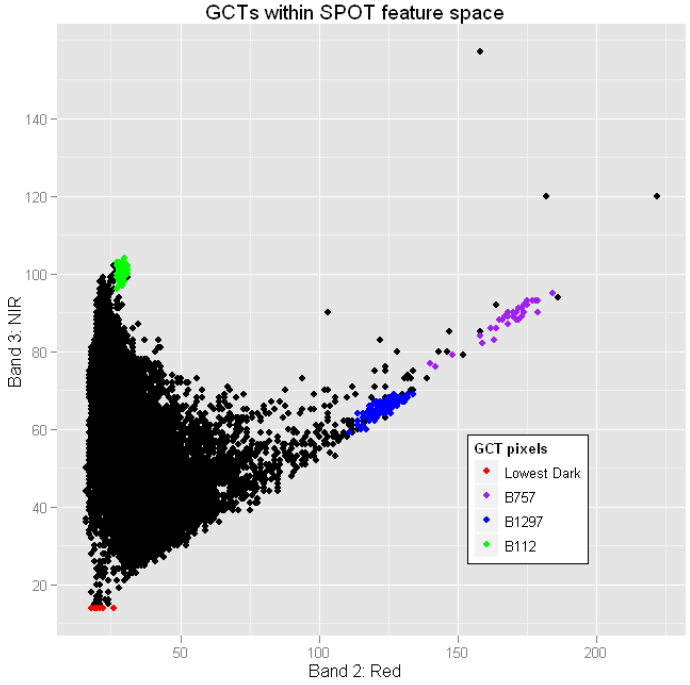

Figure 4 – Plot of NIR and Red bands showing the locations of the selected GCTs within the feature space

3.2 Light GCT

Several building roofs and one large vegetated field were selected the automated method as candidate bright GCTs. Vegetated surfaces are not ideal as GCTs but are sometimes necessary due to their unique combination of low visible reflectance and high near infra-red reflectance (e.g. Smith and Milton, 1999).

Of all the bright targets, B1297 most closely approximated a multivariate normal distribution at the SPOT HRG spatial resolution (Figure 6a). However, inspecting this target on an aerial photograph (Figure 6b) showed it to be a composite of several buildings, and therefore not suitable for use with higher resolution sensors.

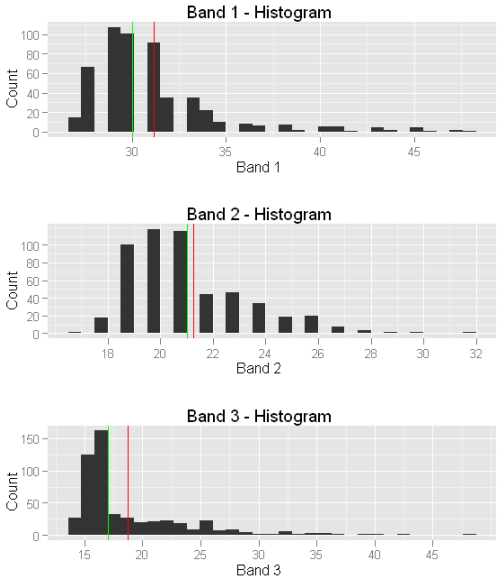

Figure 5 – Distribution of DN values from the merged dark GCT, (red line: mean, green line: median)

(a)

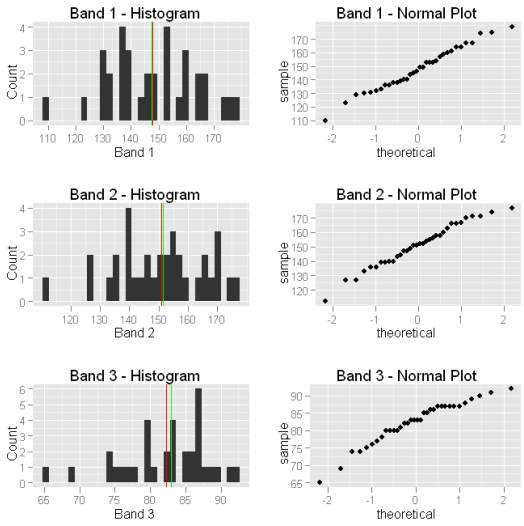

(b)

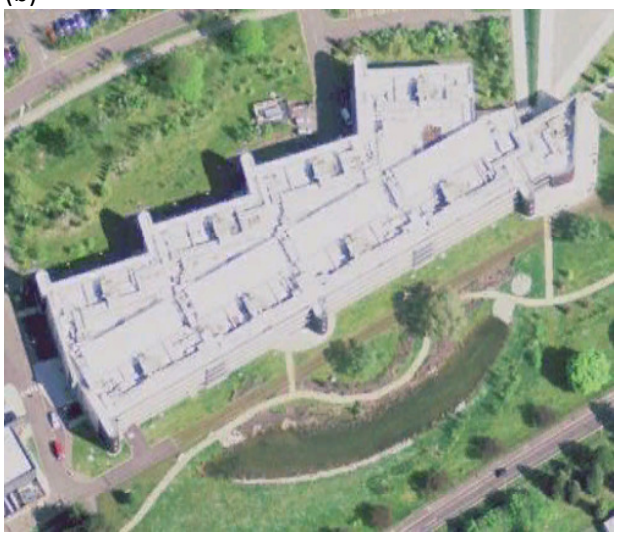

Figure 6 - (a) Distribution of DN values from GCT B1297 (red line: mean, green line: median); (b) Aerial photograph of GCT B1297 (source Google Earth, 2010)

Building roof B757 was the single best bright GCT. It had a high reflectance in all three SPOT HRG VNIR bands (as high as the vegetated field in the NIR band), and the distribution of DN values was almost normal except for a tail of dark pixels, probably due to the regular pattern of dark panels on the roof (Figure 7). As with the dark target, the median of the DN values represented the central tendency of the data better than the mean.

(a)

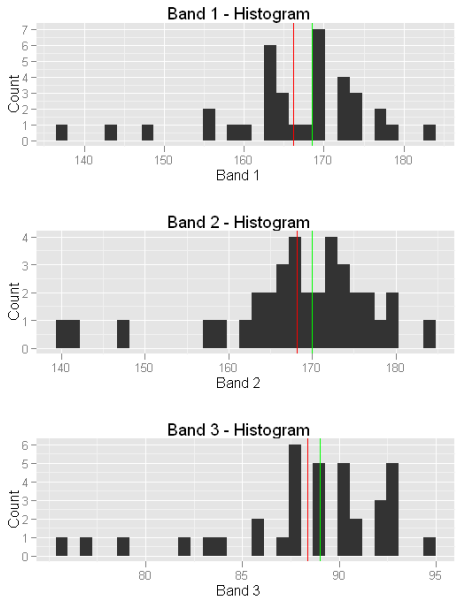

(b)

Figure 7 - (a) Distribution of DN values from GCT B757, (red line: mean, green line: median); (b) Aerial photograph of GCT B757 (source Google Earth, 2010)

5 Discussion

The method was successful in identifying a range of dark and light targets which satisfied the basic criteria outlined in Table 1. The candidate GCTs were distributed across the area of interest, and covered the complete range of brightness values in each band. Having

automatically identified the potential sites, it was necessary to study each individually to assess its suitability for use with the ELM, and to identify the single target most suitable for use with the refined ELM (Moran et al, 2001). The dark targets were all small lakes which might not be suitable at some times of the year due to high sediment load or algal blooms, and some of the bright targets were of limited value, either because they were inaccessible on the ground, or because aerial photos revealed that the roofs had vertical structures that would cast shadows at certain times of the day. However, one of the bright targets (B757) would be very suitable as a primary GCT for use with the refined ELM. The roof was very bright in all the SPOT bands, reasonably uniform even on the aerial photos, and was easily accessible on the ground (Figure 7).

One of the weaknesses of atmospheric correction methods based on ground targets concerns the spatial variability of the atmosphere, but we suggest that the method described in this paper can address this to some extent. The initial set of candidate GCTs identified by the automated method could be used to investigate spatial variation in haze across the scene, for example by studying the tasselled-cap 'yellowness' axis which has been associated with atmospheric haze (Crist, 1984). Assuming little or no variation in haze is observed, the analyst would then has greater confidence in a refined ELM correction based on field spectral measurements (BRDF) made at the primary GCT (B757).

6 Conclusion

The paper has demonstrated the potential of an automated object-based method to select candidate GCTs for atmospheric correction, but is has also shown the importance of manual screening of the selected objects. All of the GCTs selected by the automated method had potential value, whether for investigating the spatial variability of the atmosphere, as sites for use with the ELM, or as locations for detailed field measurements in support of the refined ELM. Further work will focus on refining and automating the methodology so as to provide an integrated image processing environment to support empirical image-based atmospheric correction.

7 Acknowledgements

The SPOT HRG data from the NCAVEO Field Campaign were provided by CNES, the NEXTMap data were provided by Intermap Technologies, and both were sourced via the NERC Earth Observation Data Centre (NEODC).

8 References

BANNARI, A., OMARI, K., TEILLET, P. & FEDOSEJEVS, G. (2005) Potential of Getis statistics to characterize the radiometric uniformity and stability of test sites used for the calibration of Earth observation sensors. *IEEE transactions on Geoscience and Remote Sensing,* 43**,** 12.

CANTY, M. J. & NIELSEN, A. A. (2008) Automatic radiometric normalization of multitemporal satellite imagery with the iteratively re-weighted MAD transformation. *Remote Sensing of Environment,* 112**,** 1025-1036.

CASELLES, V. & LÓPEZ GARCÍA, M. J. (1989) An alternative simple approach to estimate atmospheric correction in multitemporal studies. *International Journal of Remote Sensing,* 10**,** 1127-1134.

CLARK, R. N., SWAYZE, G. A., LIVO, K. E., KOKALY, R. F., KING, J. B., DALTON, J. S., ROCKWELL, B. W., HOEFEN, T. & MCDOUGAL, R. R. (2003) Surface Reflectance

Calibration of Terrestrial Imaging Spectroscopy Data: a Tutorial Using AVIRIS. *AVIRIS Workshop Proceedings.* http://speclab.cr.usgs.gov/PAPERS.calibration.tutorial/

CRIST, E. P. (1984) A spectral haze diagnostic feature for normalising Landsat thematic mapper data. *18th Int. Symp. on Remote Sensing of Environment, Paris, France,* 735-744.

ELVIDGE, C. D., YUAN, D., WEERACKOON, R. D. & LUNETTA, R. S. (1995) Relative radiometric normalization of Landsat Multispectral Scanner (MSS) data using an automatic scattergram-controlled regression. *Photogrammetric Engineering and Remote Sensing,* 61**,** 1255-1260.

GETIS, A. (1994) Spatial dependence and heterogeneity and proximal databases. *Spatial analysis and GIS***,** 105–120.

GRUNINGER, J., RATKOWSKI, A. & HOKE, M. (2004) The sequential maximum angle convex cone (SMACC) endmember model. *Proceedings SPIE, Algorithms for Multispectral and Hyper-spectral and Ultraspectral Imagery,* 5425**,** 1–14.

HOLM, R. G., JACKSON, R. D., YUAN, B., MORAN, M. S. & SLATER, P. N. (1989) Surface Reflectance Factor Retrieval from Thematic Mapper Data. *Remote Sensing of Environment,* 27**,** 47-57.

KARPOUZLI, E. & MALTHUS, T. J. (2003) The empirical line method for the atmospheric correction of IKONOS imagery. *International Journal of Remote Sensing,* 24**,** 1143-1150.

MILTON, E. J. & NCAVEO PARTNERSHIP, N. (2008) The Network for Calibration and Validation in Earth Observation (NCAVEO) 2006 Field Campaign. *Proceedings of the Remote Sensing and Photogrammetry Society Conference 2008, 'Measuring change in the Earth system'.* University of Exeter, Remote Sensing and Photogrammetry Society, University of Nottingham

MORAN, M. S., BRYANT, R., THOME, K. J., NI, W., NOUVELLON, Y., GONZALEZ-DUGO, M. P., QI, J. & CLARKE, T. R. (2001) A refined empirical line approach for reflectance factor retrieval from Landsat-5 TM and Landsat-7 ETM+. *Remote Sensing of Environment,* 78**,** 71-82.

SCHMIDT, M., KING, E. A. & MCVICAR, T. R. (2008) A method for operational calibration of AVHRR reflective time series data. *Remote Sensing of Environment,* 112**,** 1117-1129.

SCHOTT, J. R., SALVAGGIO, C. & VOLCHOK, W. J. (1988) Radiometric scene normalisation using pseudoinvariant features. *Remote Sensing of Environment,* 26**,** 1-16.

SMITH, G. M. & MILTON, E. J. (1999) The use of the Empirical Line Method to calibrate remotely sensed data to reflectance. *International Journal of Remote Sensing,* 20**,** 2653-2662.

THOME, K. J. (2001) Absolute radiometric calibration of Landsat 7 ETM+ using the reflectance-based method. *Remote Sensing of Environment,* 78**,** 27-38